

The fast neutron fluence and the activation monitor activity calculations using fine multigroup and continuous nuclear data

Martin Lovecký^{1,2,*}, Pavlína Tušlová¹, and Vladimír Smutný¹

¹ŠKODA JS a.s., Orlík 266, 316 00 Plzeň, Czech Republic

²Faculty of Electrical Engineering, University of West Bohemia, Univerzitní 8, 306 14 Plzeň, Czech Republic

Abstract. The fast neutron fluence and the activation monitor activities are routinely calculated with TORT deterministic code and BUGLE-B7 nuclear data library with 47 broad energy groups. The objective of the paper is to analyse options to improve reactor dosimetry transport calculations. There are two paths to improve reactor dosimetry calculations. Increasing geometry, angular and energy mesh size is applicable for TORT code while using newer nuclear data libraries is relevant for both deterministic and Monte Carlo codes. Two new calculation options (improved TORT and Monte Carlo MCNP6) were compared with the standard TORT calculation for VVER-440 Dukovany Unit 3 Cycle 31. The fast neutron fluence with 0.5 MeV threshold as well as activity of Fe, Ni, Ti, Cu, Mn and Nb monitors were evaluated. Standard TORT calculations were improved from S₁₆P₃ to S₃₀P₃ with three times finer axial mesh size, 120° core symmetry r- θ mesh size with 0.5° step and fine multigroup libraries VITAMIN-B7 with 199 neutron energy groups and ENDF/B-VII.1 with 200 neutron energy groups. Both ENDF/B and IRDFF activation cross sections were used. The drawback of expanded mesh size is raised calculation runtime since TORT deterministic code is not parallelized and one calculation can require multiple weeks of CPU time. An alternative option of using MCNP6 Monte Carlo code with continuous ENDF/B-VII.1 nuclear data with detailed 3-D geometry and pin-wise effective neutron source prepared by MOBY-DICK diffusion code reactor analysis was explored. It was found that using finer mesh size affects reactor dosimetry tallies less than the choice of nuclear data library. BUGLE-B7 and VITAMIN-B7 produce results typically within 1 % difference. ENDF/B-VII.1 calculations with 200 neutron energy groups with TORT code are even in better agreement with MCNP6 calculations with continuous nuclear data libraries. The largest differences of around 2 % were observed between VITAMIN-B7 library based on ENDF/B-VII.0 nuclear data and ENDF/B-VII.1 library. Nuclear data library has larger impact on the results with up to 7 % difference between all 0.5 MeV fast neutron fluence calculations. The largest impact of nuclear data was observed for Mn(n,2n) monitor.

* Corresponding author: martin.lovecky@skoda-js.cz

1 Calculation approaches to neutron transport

The fast neutron fluence and the activation monitor activities are routinely calculated with TORT deterministic code [7]. The objective of the paper is to analyse options to improve reactor dosimetry transport calculations. There are two paths to improve reactor dosimetry calculations. Increasing geometry, angular and energy mesh size is applicable for TORT code while using newer nuclear data libraries is relevant for both deterministic and Monte Carlo codes. Two new calculation options (improved TORT and Monte Carlo MCNP6 [8]) were compared with the standard TORT calculation for VVER-440 Dukovany Unit 3 Cycle 31. The fast neutron fluence with 0.5 MeV threshold as well as activity of Fe, Ni, Ti, Cu, Mn and Nb monitors were evaluated, see Table 1.

Table 1. Set of activation detectors used in Czech NPPs reactor dosimetry.

Reaction (-)	Half-life (d)	Gamma line energy (keV)
Fe-54(n,p)Mn-54	312.5	835
Ni-58(n,p)Co-58	70.8	811
Ti-46(n,p)Sc-46	83.83	889; 1121
Cu-63(n, α)Co-60	1925.2	1173; 1332
Mn-55(n,2n)Mn-54	312.5	835
Nb-93(n,n')Nb-93m	5890.0	16.6; 18.7

Standard TORT model is the evolution of two-dimensional geometry models in DORT code [1] that has been replaced by more precise three-dimensional geometric models in TORT code. 120 degrees azimuthal segment with periodic boundary condition is used with 180 mesh cells. Inner 60 degrees are using 0.5° cells, while the outer 30° segments are divided by 1.0° precision. Number of cells in axial dimension is 54, fuel column with neutron source is divided into 42+1 cells, 42 cells consistently with MOBY-DICK diffusion macrocode [9] that prepares neutron source [2], [3], one cell containing weld material is split into two. Radial cells with 0.3 cm to 12.0 cm width describe homogenized reactor core and heterogenous reactor internals, pressure vessel and biological shielding with ionization chambers with a total of 238 mesh cells. BUGLE-B7 library with 47 broad group energy structure based on ENDF/B-VII.0 is the newest broad group library available for TORT code. Discrete ordinates method in TORT code uses $S_{16}P_3$ approach for standard TORT model.

Improved TORT model is based on the standard TORT model, only with much finer calculational grid with increased number of mesh cells. Uniform 0.5° angular cells in 120° core segment result in 240 cells. Fuel column is divided into three times finer axial cells, axial mesh size increase from 54 to 162 cells. Fine group libraries VITAMIN-B7 from BUGLE-B7 distribution [4] and ENDF/B-VII.1 from SCALE-6.2.4 distribution [5] are both used. The first library with 199 neutron groups is based on ENDF/B-VII.0 nuclear data library while the latter uses 200 neutron groups and ENDF/B-VII.1 nuclear data. Group structure and energy boundaries are listed in BUGLE-VITAMIN documentation [4] for 199 neutron group structure and in SCALE manual [5] for 200 neutron group structure. ALPO code from SCALE code package was used to convert ENDF/B-VII.1 multipurpose nuclear data library from AMPX format used in SCALE to ANISN format used by TORT. Discrete

ordinates approach is improved to $S_{30}P_3$. Dimensions in TORT source code has been expanded to utilize larger memory demand associated with larger model meshes, however, the calculational time is enormous due to the absence of parallelism in TORT code. A single transport calculation takes around a month of wall clock time.

Monte Carlo MCNP6 model was prepared from TORT model, geometry and materials are comparable between the two codes. The reactor core contain heterogenous fuel pin and coolant regions, see Figure 1. Continuous nuclear data library is used, ENDF/B-VII.1 library is used as the best library currently available for VVER reactor dosimetry area. Newer ENDF/B-VIII.0 library is not suitable for reactor dosimetry [6]. Temperature profile in reactor internals is modelled by temperature card in MCNP6 code, the profile in the reactor core was calculated by MOBY-DICK code.

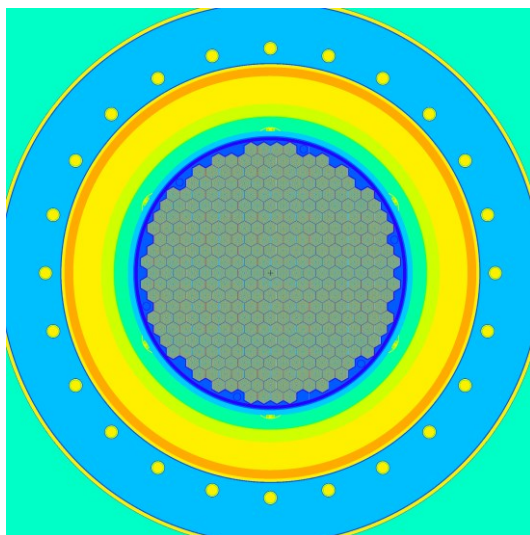


Fig. 1. VVER-440/V-213 reactor core model in MCNP6, detail in xy plane.

Activation cross sections are used from two sources. The first approach is to use the activation cross sections from the transport library used in the calculation. In the case of BUGLE-B7 library, cross sections at $\frac{1}{4}$ depth of the pressure vessel are used. The second approach is to use activation cross sections from IRDFF-II nuclear data library.

2 Neutron source

Neutron source for transport calculations in reactor dosimetry is based on diffusion calculations of a reactor core operation during a fuel cycle. In Dukovany nuclear power plant online monitoring system and safety analyses, MOBY-DICK code is being used to model operation of VVER-440 reactor. Effective neutron source method described in detail in [2] and [3] prepares time-integrated neutron source for various neutron flux functionals; namely neutron fluence and activity per nucleus (APN) for activation foils used in ex-core reactor dosimetry. Time integration takes into account power profile during operation as well as radionuclide decay to determine APN at the end of cycle. Neutron source is calculated as a product of neutron flux, macroscopic fission cross section and fission neutron yield.

An effective neutron source for neutron fluence is a time integration of neutron source during the reactor cycle. An effective neutron source for activation calculations of APN

is a time integration concerning the half-life of activated foils radionuclide that results in a lower influence of neutrons at the beginning of the fuel cycle and a higher influence of neutrons before reactor shutdown. The longer the half-life, the more minor the influence differences are.

Spatial resolution of effective neutron source is pin-wise with standard 42 uniform axial layers or finer 126 uniform layers. Each fuel cell containing one fuel pin in one axial layer is the smallest spatial resolution of the MOBY-DICK code. The diffusion code calculates number of fission neutrons emitted from the nuclear fuel for around 100 time steps that are subsequently integrated via effective neutron source method. Relative neutron source for Fe dosimetry monitor for all actinides in axial layer 20 near core midplane are plotted in Figures 2 and 3 for Dukovany Unit 3 Cycle 31.

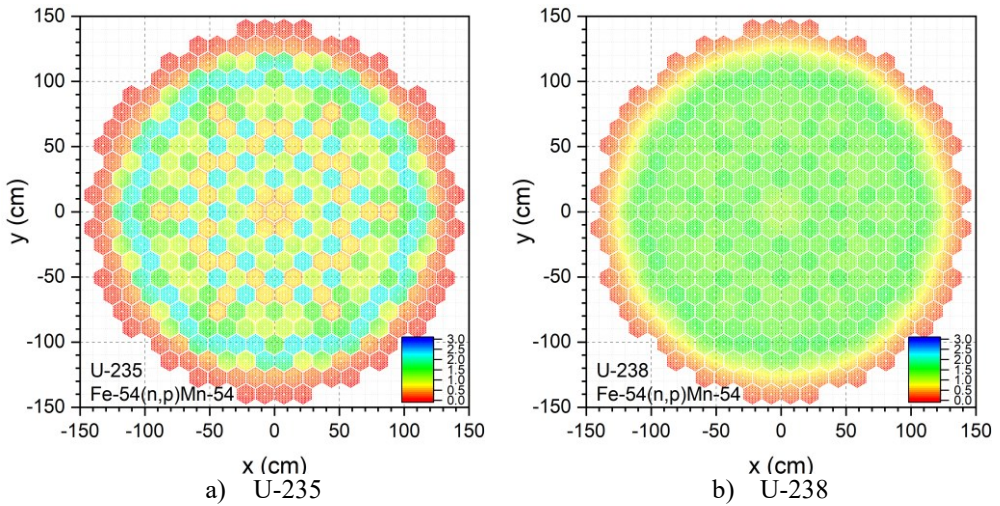


Fig. 2. Neutron source distribution for Fe monitor, uranium isotopes, relative to average source.

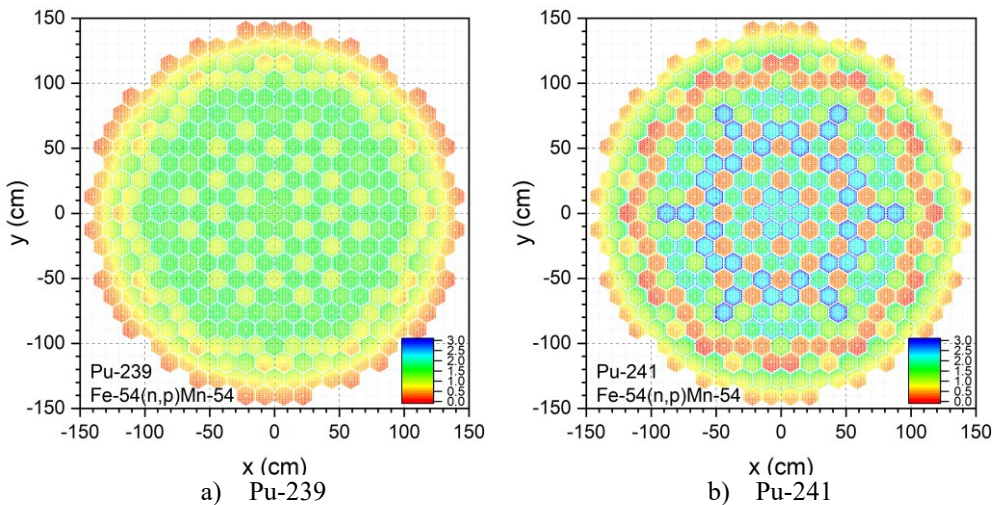


Fig. 3. Neutron source distribution for Fe monitor, plutonium isotopes, relative to average source.

Energy spectra is unique for each of the four involved actinides and are described in nuclear data libraries. U-235, U-238, Pu-239 and Pu-241 is responsible to majority of all fission neutrons in the core (tested on VVER fuel with burnup up to 85000 MWd/MTU, where maximum fraction of neutron source from other actinides is 2.1 % for Cm-245). In TORT code, each mesh cell with neutron source contains linear combination of energy spectra and source strength from the mentioned actinides in 47, 199 or 200 energy groups consistent with transport calculation.

In MCNP6 code, the calculation is split into 4 cases for each actinide, because linear combination as done in TORT code is not feasible for MCNP6 code due to limitations in different energy spectra shapes (SPn card dimension limit is 999). Number of spatial volumes with neutron source is almost 2 million (126 fuel pins, 42 axial layers, 349 fuel assemblies). To avoid source sampling issues linked to the high number of source cells, high precision simulation resulting in Monte Carlo statistical uncertainty of 0.3 % was performed.

3 Calculation results

Maximum neutron fluence in the pressure vessel was calculated at the inner surface with 177.1 cm radius at 30° azimuth in core midplane. Similarly, APN were calculated at the pressure vessel outer surface at 192.0 cm radius. Absolute results are summarized in Table 2, values for both TORT and MCNP6 calculations relative to standard TORT calculations with BUGLE-B7 are compared in Table 3. Missing values intentional to reduce overall calculation time, the differences between there cases do not impact the conclusions.

It was found that using finer mesh size affects reactor dosimetry tallies less than the choice of nuclear data library. BUGLE-B7 and VITAMIN-B7 produce results typically within 1 % difference, the largest difference of 2.5 % is for neutron fluence above 0.5 MeV.

There are differences in using ENDF-based or IRDFF activation cross sections. For the most activated monitors Fe and Ni, the differences are less than 2 %. For higher energy Ti and Cu monitors, the differences are up to 8 %. Mn monitor has high energy threshold, the results are more different in various calculation setups. Nb monitor has around 15 % difference between ENDF-based and IRDFF activation cross sections, however, IRDFF data are more suitable since Nb activation cross section in ENDF/B libraries has not been revised in either VII or VIII evaluations and IRDFF are closer to preliminary experimental results.

The choice of ENDF/B-VII.0 or ENDF/B-VII.1 nuclear data library has higher influence on the analysis results than mesh size. Differences for improved TORT with 199/200 energy groups are from 2 % to 3 % for neutron fluence, Fe, Ni and Cu monitors. Mn monitor differs around 35 % and Nb monitor around 6 %. Mn monitor differences are significant; however, the preliminary experimental results suggest neither library is better since experimental activity lies between them.

Table 2. Neutron transport absolute results for Dukovany U3C31 at 30°.

Case	Standard TORT, BUGLE-B7	Improved TORT, BUGLE-B7	Improved TORT, VITAMIN-B7	Improved TORT, ENDF/B-VII.1	MCNP6, ENDF/B-VII.1
F > 0.5 MeV (m ⁻²)	4.195E+22	4.208E+22	4.299E+22	4.427E+22	4.493E+22
F > 1.0 MeV (m ⁻²)	2.658E+22	2.603E+22	2.641E+22	2.708E+22	2.771E+22
Fe APN (Bq)	3.626E-16	3.606E-16	3.630E-16	3.709E-16	3.660E-16
Ni APN (Bq)	8.651E-16	8.569E-16	8.633E-16	8.855E-16	8.856E-16
Ti APN (Bq)	1.047E-16	1.038E-16	1.181E-16	1.033E-16	1.007E-16
Cu APN (Bq)	8.923E-19	8.885E-19	8.881E-19	8.767E-19	8.516E-19
Mn APN (Bq)	4.173E-18	4.151E-18	4.126E-18	2.684E-18	2.524E-18
Nb APN (Bq)	1.130E-16	1.118E-16	1.139E-16	1.215E-16	1.139E-16
Case	IRDF				
Fe APN (Bq)	3.553E-16	3.532E-16	—	—	3.589E-16
Ni APN (Bq)	8.552E-16	8.469E-16	—	—	8.746E-16
Ti APN (Bq)	1.121E-16	1.111E-16	—	—	1.091E-16
Cu APN (Bq)	9.165E-19	9.125E-19	—	—	8.672E-19
Mn APN (Bq)	3.746E-18	4.212E-18	—	—	2.557E-18
Nb APN (Bq)	9.862E-17	9.844E-17	1.003E-16	1.067E-16	1.139E-16

Table 3. Neutron transport relative results for Dukovany U3C31 at 30°.

Case	Standard TORT, BUGLE-B7	Improved TORT, BUGLE-B7	Improved TORT, VITAMIN-B7	Improved TORT, ENDF/B-VII.1	MCNP6, ENDF/B-VII.1
F > 0.5 MeV	1.0000	1.0031	1.0248	1.0553	1.0711
F > 1.0 MeV	1.0000	0.9793	0.9936	1.0188	1.0424
Fe APN	1.0000	0.9945	1.0011	1.0229	1.0092
Ni APN	1.0000	0.9905	0.9979	1.0236	1.0237
Ti APN	1.0000	0.9914	1.1280	0.9866	0.9616
Cu APN	1.0000	0.9957	0.9953	0.9825	0.9544
Mn APN	1.0000	0.9947	0.9887	0.6432	0.6048
Nb APN	1.0000	0.9894	1.0080	1.0752	1.0081
Case	IRDF				
Fe APN	1.0205	1.0149	—	—	1.0300
Ni APN	1.0116	1.0020	—	—	1.0356
Ti APN	0.9340	0.9260	—	—	0.8982
Cu APN	0.9736	0.9694	—	—	0.9292
Mn APN	1.1140	1.1081	—	—	0.6737
Nb APN	1.1458	1.1336	1.1549	1.2320	1.1551

Because MCNP6 calculation was performed separately for each of the four actinides, it is possible to compare source strength with contribution to the results. Effective neutron source strengths are compared in Table 4. U-235 typically accounts for 50 % of source neutrons, U-238 and Pu-241 around 8 % each and the remaining 1/3 of neutrons has Pu-239 spectra. However, due to different spatial and energy distribution, contribution of U-235 drops to interval between 19 % and 29 %, see Table 5. Around 50 % of neutron fluence and APN are contributed from Pu-239 neutrons. The reason to evaluate the contribution of each actinide is that different neutron energy spectra are emitted from the fission at the actinides, and plutonium has harder spectra and higher strength at the core periphery close to the pressure vessel.

Table 4. Effective neutron source strength contributions.

Case	U-235	U-238	Pu-239	Pu-241
fluence	0.4959	0.0791	0.3512	0.0739
Fe	0.4822	0.0789	0.3616	0.0772
Ni	0.4482	0.0786	0.3871	0.0860
Ti	0.4532	0.0787	0.3835	0.0847
Cu	0.4936	0.0790	0.3529	0.0744
Mn	0.4822	0.0789	0.3616	0.0772
Nb	0.4952	0.0790	0.3517	0.0741

Table 5. Neutron fluence and APN contributions.

Case	U-235	U-238	Pu-239	Pu-241
F 0.5 MeV	0.2841	0.0736	0.4949	0.1473
F 1.0 MeV	0.2855	0.0730	0.4945	0.1470
Fe	0.2832	0.0697	0.4983	0.1488
Ni	0.2686	0.0687	0.5087	0.1541
Ti	0.2670	0.0656	0.5087	0.1587
Cu	0.2806	0.0646	0.4962	0.1586
Mn	0.1912	0.0427	0.4953	0.2708
Nb	0.2900	0.0727	0.4917	0.1456

4 Conclusions

Two paths to improve reactor dosimetry calculations were analysed for reactor dosimetry for Dukovany Unit 31 Cycle 31. Increasing geometry, angular and energy mesh size is applicable for TORT code while using newer nuclear data libraries is relevant for both deterministic and Monte Carlo codes.

It was found that using finer mesh size affects reactor dosimetry tallies less than the choice of nuclear data library. BUGLE-B7 and VITAMIN-B7 produce results typically within 1 % difference. ENDF/B-VII.1 calculations with 200 neutron energy groups with TORT code are even in better agreement with MCNP6 calculations with continuous nuclear data libraries. The largest differences of around 2 % were observed between VITAMIN-B7 library based on ENDF/B-VII.0 nuclear data and ENDF/B-VII.1 library. Nuclear data library has larger impact on the results with up to 7 % difference between all 0.5 MeV fast neutron fluence calculations. The largest impact of nuclear data was observed for Mn(n,2n) monitor.

References

1. K. Ilieva, T. Apostolov, S. Belousov, I. Penev, I. Popova, *Validation of Neutron Fluence Calculation Methodology for VVER-440 Vessel*, Nuclear Science and Engineering **125** (1996)
2. V. Smutný, A. Konečná, D. Sprinzl, V. Klupák, M. Vinš, *The Activation Detector Activity Calculations Using the Effective Source Method and Measurement*, EPJ Web of Conferences **153** (2017)
3. J. Hep, A. Konečná, V. Krýsl, V. Smutný, *The Fast Neutron Fluence and the Activation Detector Activity Calculations Using the Effective Source Method and the Adjoint Function*, Journal of ASTM International **9** (2012)
4. *BUGLE-B7/VITAMIN-B7: Broad-Group and Fine-Group and Coupled Neutron/Gamma Cross-Section Libraries Derived from ENDF/B-VII.0 Nuclear Data*, DLC-245, RSICC, ORNL, Oak Ridge, Tennessee, 2011
5. B. T. Rearden, M.A. Jessee, *SCALE Code System*, ORNL/TM-2005/39, Version 6.2.4, Oak Ridge National Laboratory, Oak Ridge, Tennessee (2017)
6. M. Lovecký, K. Gincelová, P. Haroková, J. Jiříčková, V. Smutný, J. Závorka, *Performance of ENDF/B-VIII.0 library for VVER reactors criticality safety, fuel depletion and reactor dosimetry applications*, Annals of Nuclear Energy **148** (2020)
7. *DOORS 3.2a: Program Package for One, Two and Three Dimensional Discrete Ordinates Transport*, CCC-650, RSICC, ORNL, Oak Ridge, Tennessee, 2003
8. D. B. Pelowitz: *MCNP6 User's Manual*, Version 1. Los Alamos National Laboratory, Report LACP- 13-00634, Revision 0, Los Alamos, 2013
9. C. Guler, S. Levine, K. Ivanov, J. Svarny, V. Krysl, P. Mikolas, J. Sustek, *Development of the VVER core loading optimization system*, Annals of Nuclear Energy **31** (2004)